

# On the NLO QCD corrections to Higgs production and decay in the MSSM

G. Degrassi<sup>a,b</sup> and P. Slavich<sup>a,c</sup>

<sup>a</sup> *CERN, Theory Division, CH-1211 Geneva 23, Switzerland*

<sup>b</sup> *Dipartimento di Fisica, Università di Roma Tre and INFN, Sezione di Roma Tre  
Via della Vasca Navale 84, I-00146 Rome, Italy*

<sup>c</sup> *LAPTH, 9, Chemin de Bellevue, F-74941 Annecy-le-Vieux, France*

## Abstract

We present explicit analytic results for the two-loop top/stop/gluino contributions to the cross section for the production of CP-even Higgs bosons via gluon fusion in the MSSM, under the approximation of neglecting the Higgs boson mass with respect to the masses of the particles circulating in the loops. The results are obtained employing the low-energy theorem for Higgs interactions adapted to the case of particle mixing. We discuss the validity of the approximation used by computing the first-order correction in an expansion in powers of the Higgs boson mass. We find that, for the lightest CP-even Higgs boson, the gluino contribution is very well approximated by the result obtained in the limit of vanishing Higgs mass. As a byproduct of our calculation, we provide results for the two-loop QCD contributions to the photonic Higgs decay.

---

e-mail:  
degrassi@fis.uniroma3.it  
Pietro.Slavich@cern.ch

# 1 Introduction

One of the main goals of the present experimental program at the Tevatron and at the Large Hadron Collider (LHC) is the search for the Higgs boson(s) in order to elucidate the mechanism of electroweak symmetry breaking. To support this goal, an accurate theoretical knowledge of the Higgs production cross-section, its decay modes, and the important background processes is required (for a general review see ref. [1]).

In the Standard Model (SM) the minimal realization of the Higgs sector predicts a single neutral Higgs boson  $H_{\text{SM}}$ , whose mass can be constrained by electroweak precision data and the direct-search limit from LEP to be lighter than roughly 200 GeV. At LHC the main production mechanism for  $H_{\text{SM}}$  is the loop-induced gluon fusion mechanism [2],  $gg \rightarrow H_{\text{SM}}$ , where the coupling of the gluons to the Higgs is mediated by loops of colored fermions, primarily the top quark. The knowledge of this process in the SM includes the full next-to-leading order (NLO) QCD corrections [3, 4], the next-to-next-to-leading order (NNLO) QCD corrections in the limit of infinite top mass [5], soft-gluon resummation effects [6], an estimate of the next-to-next-to-next-to-leading order (NNNLO) QCD effects [7] and also the first-order electroweak corrections [8, 9].

The Minimal Supersymmetric extension of the Standard Model, or MSSM, features a richer Higgs spectrum that consists of two neutral CP-even bosons  $h, H$ , one neutral CP-odd boson  $A$  and two charged scalars  $H^\pm$ . As in the SM, the gluon-fusion process is the main production mechanism for the neutral Higgs bosons. Furthermore, in the MSSM, the coupling of the gluons to the Higgs bosons is mediated not only by colored fermions but also by their supersymmetric partners. Thus, the study of the NLO QCD corrections to the cross section for Higgs boson production via gluon fusion in the MSSM requires the investigation of a larger variety of diagrams with respect to the SM case. Two-loop diagrams involving squarks and gluons were first considered in ref. [10] under the assumption that the Higgs boson mass can be neglected w.r.t. the masses of the particles running in the loops. Later this approximation has been relaxed and the full dependence on all the relevant masses has been retained [11, 12, 13]. Explicit two-loop results for the diagrams that involve quarks, squarks and gluinos, as well as for the diagrams that involve the D-term-induced quartic squark couplings, have been presented so far only in the limit of vanishing Higgs mass. Indeed, ref. [14] provided analytic formulae for the contributions involving top quark and/or stop squarks, valid for vanishing Higgs mass and under the additional simplifying limits of zero stop mixing and hierarchical patterns of soft SUSY-breaking masses. Ref. [15] presented a computation of the same contributions valid for arbitrary parameters in the stop sector. However, the explicit results were too long to be printed, and were made available only in the form of a computer code. Recently, the rather daunting calculation of the full two-loop QCD Higgs-gluon-gluon amplitude in the MSSM for arbitrary Higgs mass has been completed [16]. The calculation relies on a combination of analytical and numerical methods, and explicit results have not been made available so far.

Given the importance of the Higgs-physics search program, it is highly desirable to have the NLO radiative corrections to the gluon-fusion cross section expressed in a simple and flexible analytic form

that can be easily used to investigate large regions of the MSSM parameter space. To this purpose, we present explicit analytic results for the two-loop top/stop/gluino contributions to the cross section for CP-even Higgs boson production, under the approximation of neglecting the Higgs mass with respect to the masses of the particles circulating into the loops. Our results were obtained by adapting the low-energy theorem for Higgs interactions [17] to the case of particle mixing. We confirm the result of ref. [15] by a numerical comparison, after accounting for the different renormalization scheme adopted in that paper. We then discuss the validity of the approximation of vanishing Higgs boson mass by computing the first correction to it, i.e. terms of  $\mathcal{O}(m_h^2/M^2)$  where  $M$  is the generic mass of the particles circulating in the loop. We show that, for the lightest Higgs boson  $h$ , the gluino contribution is very well approximated by the result obtained in the limit of vanishing Higgs mass. As a byproduct of our calculation, we provide results for the two-loop QCD contributions to the photonic Higgs decay.

The paper is organized as follows: in section 2 we summarize general results on the cross section for Higgs boson production via gluon fusion. In section 3 we describe our calculation of the two-loop contributions to the CP-even Higgs-gluon-gluon form factors. In section 4 we assess the validity of the approximation of vanishing Higgs mass. In section 5 we explain how to adapt our results to the calculation of the gluonic and photonic decay widths of the Higgs bosons. In section 6 we discuss the applicability to other processes of our way to compute the SUSY-QCD corrections. Finally, in the appendix we provide the explicit analytical results for the two-loop top/stop/gluino contributions to the Higgs-gluon-gluon form factors.

## 2 Higgs production via gluon fusion at NLO in the MSSM

In this section we summarize some general results on Higgs boson production via gluon fusion. The hadronic cross section for Higgs boson production at center-of-mass energy  $\sqrt{s}$  can be written as

$$\sigma(h_1 + h_2 \rightarrow \phi + X) = \sum_{a,b} \int_0^1 dx_1 dx_2 f_{a,h_1}(x_1, \mu_F) f_{b,h_2}(x_2, \mu_F) \times \int_0^1 dz \delta\left(z - \frac{\tau_\phi}{x_1 x_2}\right) \hat{\sigma}_{ab}(z), \quad (1)$$

where  $\phi = (h, H)$ ,  $\tau_\phi = m_\phi^2/s$ ,  $\mu_F$  is the factorization scale,  $f_{a,h_i}(x, \mu_F)$ , the parton density of the colliding hadron  $h_i$  for the parton of type  $a$ , ( $a = g, q, \bar{q}$ ) and  $\hat{\sigma}_{ab}$  the cross section for the partonic subprocess  $ab \rightarrow \phi + X$  at the center-of-mass energy  $\hat{s} = x_1 x_2 s = m_\phi^2/z$ . The latter can be written in terms of the leading-order (LO) contribution  $\sigma^{(0)}$  as

$$\hat{\sigma}_{ab}(z) = \sigma^{(0)} z G_{ab}(z). \quad (2)$$

We consider now the production of the lightest CP-even Higgs boson,  $h$ , through gluon fusion. The LO term can be written as

$$\sigma^{(0)} = \frac{G_\mu \alpha_s^2(\mu_R)}{128 \sqrt{2} \pi} \left| T_F \left( -\sin \alpha \mathcal{H}_1^{1\ell} + \cos \alpha \mathcal{H}_2^{1\ell} \right) \right|^2, \quad (3)$$

where  $G_\mu$  is the muon decay constant,  $\alpha_s(\mu_R)$  is the strong gauge coupling expressed in the  $\overline{\text{MS}}$  renormalization scheme at the scale  $\mu_R$ ,  $T_F = 1/2$  is a color factor, and  $\alpha$  is the mixing angle in

the CP-even Higgs sector of the MSSM.  $\mathcal{H}_i$  ( $i = 1, 2$ ) are the form factors for the coupling of the neutral, CP-even component of the Higgs doublet  $H_i$  with two gluons, which we decompose in one- and two-loop parts as

$$\mathcal{H}_i = \mathcal{H}_i^{1\ell} + \frac{\alpha_s}{\pi} \mathcal{H}_i^{2\ell} + \mathcal{O}(\alpha_s^2). \quad (4)$$

The coefficient function  $G_{ab}(z)$  in eq. (2) can in turn be decomposed, up to NLO terms, as

$$G_{ab}(z) = G_{ab}^{(0)}(z) + \frac{\alpha_s}{\pi} G_{ab}^{(1)}(z) + \mathcal{O}(\alpha_s^2), \quad (5)$$

with the LO contribution given only by the gluon-fusion channel:

$$G_{ab}^{(0)}(z) = \delta(1-z) \delta_{ag} \delta_{bg}. \quad (6)$$

The NLO terms include, besides the  $gg$  channel, also the one-loop induced processes  $gq \rightarrow qh$  and  $q\bar{q} \rightarrow gh$ :

$$\begin{aligned} G_{gg}^{(1)}(z) &= \delta(1-z) \left[ C_A \frac{\pi^2}{3} + \beta_0 \ln \left( \frac{\mu_R^2}{\mu_F^2} \right) + \left( \frac{-\sin \alpha \mathcal{H}_1^{2\ell} + \cos \alpha \mathcal{H}_2^{2\ell}}{-\sin \alpha \mathcal{H}_1^{1\ell} + \cos \alpha \mathcal{H}_2^{1\ell}} + \text{h.c.} \right) \right] \\ &+ P_{gg}(z) \ln \left( \frac{\hat{s}}{\mu_F^2} \right) + C_A \frac{4}{z} (1-z+z^2)^2 \mathcal{D}_1(z) + C_A \mathcal{R}_{gg}, \end{aligned} \quad (7)$$

$$G_{q\bar{q}}^{(1)}(z) = \mathcal{R}_{q\bar{q}}, \quad G_{gq}^{(1)}(z) = P_{gq}(z) \left[ \ln(1-z) + \frac{1}{2} \ln \left( \frac{\hat{s}}{\mu_F^2} \right) \right] + \mathcal{R}_{gq}, \quad (8)$$

where the LO Altarelli-Parisi splitting functions are

$$P_{gg}(z) = 2C_A \left[ \mathcal{D}_0(z) + \frac{1}{z} - 2 + z(1-z) \right], \quad P_{gq}(z) = C_F \frac{1+(1-z)^2}{z}. \quad (9)$$

In the equations above,  $C_A = N_c$  and  $C_F = (N_c^2 - 1)/(2N_c)$  ( $N_c$  being the number of colors),  $\beta_0 = (11C_A - 2N_f)/6$  ( $N_f$  being the number of active flavors) is the one-loop  $\beta$ -function of the strong coupling in the SM, and

$$\mathcal{D}_i(z) = \left[ \frac{\ln^i(1-z)}{1-z} \right]_+. \quad (10)$$

The  $gg$ -channel contribution, eq. (7), involves two-loop virtual corrections to  $gg \rightarrow h$  and one-loop real corrections from  $gg \rightarrow hg$ . The former, regularized by the infrared singular part of the real emission cross section, are displayed in the first row of eq. (7). The second row contains the non-singular contribution from the real gluon emission in the gluon fusion process. The function  $\mathcal{R}_{gg}$  is obtained from one-loop diagrams where only quarks or squarks circulate into the loop, and in the limit in which the Higgs boson is much lighter than the particles in the loop it goes to  $\mathcal{R}_{gg} \rightarrow -11(1-z)^3/(6z)$ . Similarly, the functions  $\mathcal{R}_{q\bar{q}}$  and  $\mathcal{R}_{gq}$  in eq. (8) describe the  $q\bar{q} \rightarrow hg$  annihilation channel and the quark-gluon scattering channel, respectively. They are obtained from one-loop quark and squark diagrams, and in the light-Higgs limit they go to  $\mathcal{R}_{q\bar{q}} \rightarrow 32(1-z)^3/(27z)$ ,  $\mathcal{R}_{gq} \rightarrow 2z/3 - (1-z)^2/z$ .

The functions  $\mathcal{R}_{gg}$ ,  $\mathcal{R}_{q\bar{q}}$ ,  $\mathcal{R}_{qq}$  are actually completely known. Their expressions can be obtained from the results of ref. [18] (see also refs. [19, 20]).

The one-loop form factors  $\mathcal{H}_1^{1\ell}$  and  $\mathcal{H}_2^{1\ell}$  contain contributions from diagrams involving quarks or squarks. The two-loop form factors  $\mathcal{H}_1^{2\ell}$  and  $\mathcal{H}_2^{2\ell}$  contain contributions from diagrams involving quarks, squarks, gluons and gluinos. Focusing on the contributions involving the third-generation quarks and squarks, and exploiting the structure of the Higgs-quark-quark and Higgs-squark-squark couplings, we can write to all orders in the strong interactions

$$\mathcal{H}_1 = \lambda_t \left[ m_t \mu s_{2\theta_t} F_t + m_Z^2 s_{2\beta} D_t \right] + \lambda_b \left[ m_b A_b s_{2\theta_b} F_b + 2m_b^2 G_b + 2m_Z^2 c_\beta^2 D_b \right], \quad (11)$$

$$\mathcal{H}_2 = \lambda_b \left[ m_b \mu s_{2\theta_b} F_b - m_Z^2 s_{2\beta} D_b \right] + \lambda_t \left[ m_t A_t s_{2\theta_t} F_t + 2m_t^2 G_t - 2m_Z^2 s_\beta^2 D_t \right]. \quad (12)$$

In the equations above  $\lambda_t = 1/\sin\beta$  and  $\lambda_b = 1/\cos\beta$ , where  $\tan\beta \equiv v_2/v_1$  is defined as the ratio of the vacuum expectation values (vev) of the neutral components of the two Higgs doublets. Also,  $\mu$  is the higgsino mass parameter in the MSSM superpotential,  $A_q$  (for  $q = t, b$ ) are the soft SUSY-breaking Higgs-squark-squark couplings and  $\theta_q$  are the left-right squark mixing angles (here and thereafter we use the notation  $s_\varphi \equiv \sin\varphi$ ,  $c_\varphi \equiv \cos\varphi$  for a generic angle  $\varphi$ ). The functions  $F_q$  and  $G_q$  appearing in eqs. (11) and (12) denote the contributions controlled by the third-generation Yukawa couplings, while  $D_q$  denotes the contribution controlled by the electroweak, D-term-induced Higgs-squark-squark couplings. The latter can be decomposed as

$$D_q = \frac{I_{3q}}{2} \tilde{G}_q + c_{2\theta_{\tilde{q}}} \left( \frac{I_{3q}}{2} - Q_q s_{\theta_W}^2 \right) \tilde{F}_q, \quad (13)$$

where  $I_{3q}$  denotes the third component of the electroweak isospin of the quark  $q$ ,  $Q_q$  is the electric charge and  $\theta_W$  is the Weinberg angle.

The one-loop functions entering  $\mathcal{H}_i^{1\ell}$  are

$$F_q^{1\ell} = \tilde{F}_q^{1\ell} = \frac{1}{2} \left[ \frac{1}{m_{\tilde{q}_1}^2} \mathcal{G}_0^{1\ell}(\tau_{\tilde{q}_1}) - \frac{1}{m_{\tilde{q}_2}^2} \mathcal{G}_0^{1\ell}(\tau_{\tilde{q}_2}) \right], \quad (14)$$

$$G_q^{1\ell} = \frac{1}{2} \left[ \frac{1}{m_{\tilde{q}_1}^2} \mathcal{G}_0^{1\ell}(\tau_{\tilde{q}_1}) + \frac{1}{m_{\tilde{q}_2}^2} \mathcal{G}_0^{1\ell}(\tau_{\tilde{q}_2}) + \frac{1}{m_q^2} \mathcal{G}_{1/2}^{1\ell}(\tau_q) \right], \quad (15)$$

$$\tilde{G}_q^{1\ell} = \frac{1}{2} \left[ \frac{1}{m_{\tilde{q}_1}^2} \mathcal{G}_0^{1\ell}(\tau_{\tilde{q}_1}) + \frac{1}{m_{\tilde{q}_2}^2} \mathcal{G}_0^{1\ell}(\tau_{\tilde{q}_2}) \right], \quad (16)$$

where  $\tau_k \equiv 4m_k^2/m_h^2$ , and the functions  $\mathcal{G}_0^{1\ell}$  and  $\mathcal{G}_{1/2}^{1\ell}$  read

$$\mathcal{G}_0^{1\ell}(\tau) = \tau \left[ 1 + \frac{\tau}{4} \log^2 \left( \frac{\sqrt{1-\tau}-1}{\sqrt{1-\tau}+1} \right) \right], \quad (17)$$

$$\mathcal{G}_{1/2}^{1\ell}(\tau) = -2\tau \left[ 1 - \frac{1-\tau}{4} \log^2 \left( \frac{\sqrt{1-\tau}-1}{\sqrt{1-\tau}+1} \right) \right]. \quad (18)$$

The analytic continuations are obtained with the replacement  $m_h^2 \rightarrow m_h^2 + i\epsilon$ . For later convenience, we remark that in the limit in which the Higgs boson mass is much smaller than the mass of the

particle running in the loop, i.e.  $\tau \gg 1$ , the functions  $\mathcal{G}_0^{1\ell}$  and  $\mathcal{G}_{1/2}^{1\ell}$  behave as

$$\mathcal{G}_0^{1\ell} \rightarrow -\frac{1}{3} - \frac{8}{45\tau} + \mathcal{O}(\tau^{-2}), \quad \mathcal{G}_{1/2}^{1\ell} \rightarrow -\frac{4}{3} - \frac{14}{45\tau} + \mathcal{O}(\tau^{-2}). \quad (19)$$

The discussion above has focused on the production of the lightest CP-even Higgs mass-eigenstate  $h$ , whose mass is bounded at tree-level by the  $Z$ -boson mass and can hardly exceed 130–140 GeV when radiative corrections are taken into account (see, e.g., ref. [21]). In this mass range, it can be expected that the exact values of the functions  $\mathcal{H}_1^{2\ell}$  and  $\mathcal{H}_2^{2\ell}$  are well approximated by the results computed in the limit in which the  $h$  boson mass is neglected w.r.t. the masses of the particles running in the loops, which we are going to call the vanishing Higgs-mass limit (VHML). In the next section we derive explicit analytic results for the two-loop top/stop contributions to  $\mathcal{H}_1^{2\ell}$  and  $\mathcal{H}_2^{2\ell}$  in the VHML, and in section 4 we further elaborate on the validity of the approximation. For what concerns the heaviest eigenstate  $H$ , general formulae for the production cross-section can be obtained straightforwardly with the replacements ( $-\sin\alpha \rightarrow \cos\alpha$ ,  $\cos\alpha \rightarrow \sin\alpha$ ) in eqs. (3) and (7). However, depending on the choice of MSSM parameters, it might not be possible to rely on the assumption that  $H$  is much lighter than the particles running in the loops.

### 3 Explicit two-loop results in the vanishing Higgs-mass limit

In this section we derive explicit and (relatively) compact formulae, valid for arbitrary parameters in the stop sector, for the contributions of two-loop diagrams involving top quarks and/or stop squarks to the form factors for the interaction of a CP-even Higgs boson with two gluons in the VHML. Besides providing an independent check of the results of ref. [15], our formulae can be easily modified to allow for different renormalization schemes for the input parameters. Furthermore we discuss how our results for the contributions involving the stop squarks can be adapted to the squarks of other flavors.

#### 3.1 Derivation of the two-loop top/stop contributions

The starting point of our derivation is the low-energy theorem (LET) for Higgs interactions [17] (see also ref. [22]), relating the amplitude  $\mathcal{M}(X, \phi)$  for a generic particle configuration  $X$  plus an external Higgs boson  $\phi$  of vanishing momentum to the corresponding amplitude without the external Higgs boson,  $\mathcal{M}(X)$ . The LET can be stated as follows: the amplitude  $\mathcal{M}(X, \phi)$  can be obtained by considering  $\mathcal{M}(X)$  as a field-dependent quantity via the dependence of the relevant parameters (masses and mixing angles) on  $\phi$ . The first term in the expansion of  $\mathcal{M}(X)$  in the Higgs field, evaluated at the minimum of the Higgs potential, corresponds to  $\mathcal{M}(X, \phi)$ . Strictly speaking, in case  $\mathcal{M}(X)$  contains infrared (IR) divergent terms the theorem applies to the IR-safe part of the two amplitudes. If  $\phi$  represents a pseudoscalar Higgs boson and  $X$  a pair of vector bosons, an additional contribution to  $\mathcal{M}(X, \phi)$  is induced by the axial-current anomaly. This contribution cannot be expressed in terms of derivatives of  $\mathcal{M}(X)$  and must be computed explicitly.

To derive the CP-even Higgs-gluon-gluon form factors in the VHML we apply the LET, identifying  $\mathcal{M}(X)$  with the gluon self-energy in the background-field gauge [23]. Then, the top/stop contributions to the form factors  $\mathcal{H}_i$  ( $i = 1, 2$ ) are given by

$$\mathcal{H}_i \Big|_{m_\phi^2=0}^{\text{top/stop}} = \frac{2\pi v}{\alpha_s T_F} \frac{\partial \Pi^t(0)}{\partial S_i}, \quad (20)$$

where  $v \equiv v_1^2 + v_2^2 \approx 246$  GeV is the electroweak symmetry breaking parameter,  $S_i$  ( $i = 1, 2$ ) are the CP-even parts of the neutral components of the two MSSM Higgs doublets and  $\Pi^t(q^2)$  denotes the top/stop contribution to the transverse part of the adimensional (i.e. divided by  $q^2$ ) self-energy of the gluon. In analogy with the discussion in ref. [24], the dependence of the latter on the Higgs fields  $S_i$  can be identified through the field dependence of the top and stop masses and of the stop mixing angle. The self-energy depends also upon a fifth field-dependent parameter related to the phase difference between the top and stop fields. However, this parameter is relevant only when one consider derivatives with respect to the CP-odd fields, thus it can be ignored in our case. As in ref. [24], a lengthy but straightforward application of the chain rule allows us to express the functions  $F_t$ ,  $G_t$ ,  $\tilde{F}_t$  and  $\tilde{G}_t$  appearing in eqs. (11, 12) and in eq. (13) as combinations of the derivatives of the gluon self-energy with respect to the top and stop masses and to the stop mixing angle. In particular, we find for the two-loop parts of the functions

$$F_t^{2\ell} = \frac{\partial Z}{\partial m_{\tilde{t}_1}^2} - \frac{\partial Z}{\partial m_{\tilde{t}_2}^2} - \frac{4 c_{2\theta_t}^2}{m_{\tilde{t}_1}^2 - m_{\tilde{t}_2}^2} \frac{\partial Z}{\partial c_{2\theta_t}^2}, \quad (21)$$

$$G_t^{2\ell} = \frac{\partial Z}{\partial m_{\tilde{t}_1}^2} + \frac{\partial Z}{\partial m_{\tilde{t}_2}^2} + \frac{\partial Z}{\partial m_t^2}, \quad (22)$$

$$\tilde{F}_t^{2\ell} = \frac{\partial Z}{\partial m_{\tilde{t}_1}^2} - \frac{\partial Z}{\partial m_{\tilde{t}_2}^2} + \frac{4 s_{2\theta_t}^2}{m_{\tilde{t}_1}^2 - m_{\tilde{t}_2}^2} \frac{\partial Z}{\partial c_{2\theta_t}^2}, \quad (23)$$

$$\tilde{G}_t^{2\ell} = \frac{\partial Z}{\partial m_{\tilde{t}_1}^2} + \frac{\partial Z}{\partial m_{\tilde{t}_2}^2}, \quad (24)$$

where, to reduce clutter, we used the shortcut  $Z \equiv (2/T_F)\Pi^{2\ell,t}(0)$ , after decomposing the gluon self-energy in one- and two-loop parts as

$$\Pi(q^2) = \frac{\alpha_s}{\pi} \Pi^{1\ell}(q^2) + \left(\frac{\alpha_s}{\pi}\right)^2 \Pi^{2\ell}(q^2) + \mathcal{O}(\alpha_s^3). \quad (25)$$

We computed the contributions to the gluon self-energy from the two-loop diagrams that involve top and/or stops with the help of **FeynArts** [25], using a version of the MSSM model file adapted to the background field gauge. After isolating the transverse part of the self-energy with a suitable projector, we Taylor-expanded it in powers of the squared external momentum  $q^2$ . The zeroth-order term of the expansion vanishes as a consequence of gauge invariance, while the first-order term corresponds indeed to  $\Pi^{2\ell,t}(0)$ . We evaluated the two-loop vacuum integrals using the results of ref. [26]. Finally, we computed all the derivatives<sup>1</sup> of  $Z$  that enter eqs. (21)–(24).

<sup>1</sup>In ref. [26] the two-loop vacuum integrals are expressed in terms of a function  $\Phi(m_1^2, m_2^2, m_3^2)$ , whose derivatives can be easily obtained using the results of appendix A of ref. [27].

We performed the two-loop computation using dimensional regularization (DREG) and modified minimal subtraction ( $\overline{\text{MS}}$ ). However, it is convenient to express our results in terms of parameters renormalized in the  $\overline{\text{DR}}$  scheme, which is based on dimensional reduction (DRED) and preserves the supersymmetric Ward identities and relations. The conversion of the parameters from the  $\overline{\text{MS}}$  scheme to the  $\overline{\text{DR}}$  scheme was discussed in ref. [28]. In particular, the  $\overline{\text{DR}}$  Higgs-quark-quark Yukawa couplings differ from their  $\overline{\text{MS}}$  counterparts by a finite one-loop shift which, when inserted in the one-loop part of a calculation, induces an additional two-loop contribution. On the other hand, the couplings of the Higgs bosons to squarks, as far as strong corrections are concerned, are the same in both schemes, and they are related by supersymmetry to the corresponding  $\overline{\text{DR}}$  Yukawa couplings. Specializing to our calculation, only the top contribution to  $\mathcal{H}_2^{1\ell}$  is going to induce an additional two-loop contribution when the top Yukawa coupling is converted from its  $\overline{\text{MS}}$  value to its  $\overline{\text{DR}}$  value, while the stop contributions to  $\mathcal{H}_1^{1\ell}$  and  $\mathcal{H}_2^{1\ell}$  can be directly identified as expressed in terms of  $\overline{\text{DR}}$  parameters. However, as can be seen from eqs. (12, 15, 19), in the VHML the top-quark contribution to  $\mathcal{H}_2^{1\ell}$  goes to a constant, i.e. it does not actually depend on the top Yukawa coupling. Therefore we need not introduce any additional contribution<sup>2</sup> to the two-loop results obtained using DREG.

In the explicit formulae for the derivatives of  $Z$  we identify the contributions of diagrams with gluons ( $g$ ), with strong, D-term-induced quartic stop couplings ( $4\tilde{t}$ ), and with gluinos ( $\tilde{g}$ ). Assuming that the parameters in  $\mathcal{H}_1^{1\ell}$  and  $\mathcal{H}_2^{1\ell}$  are expressed in the  $\overline{\text{DR}}$  scheme, the non-vanishing contributions of the two-loop diagrams with gluons read

$$\frac{\partial Z^g}{\partial m_{\tilde{t}}^2} = \frac{1}{2m_{\tilde{t}}^2} \left( C_F - \frac{5C_A}{3} \right), \quad (26)$$

$$\frac{\partial Z^g}{\partial m_{\tilde{t}_i}^2} = -\frac{1}{2m_{\tilde{t}_i}^2} \left( \frac{3C_F}{4} + \frac{C_A}{6} \right), \quad (27)$$

where  $i = 1, 2$ . Under the same assumption for the renormalization of the input parameters, the non-vanishing contributions of the two-loop diagrams that involve strong quartic stop couplings read

$$\frac{\partial Z^{4\tilde{t}}}{\partial m_{\tilde{t}_1}^2} = -\frac{C_F}{24} \left[ \frac{c_{2\theta_t}^2 m_{\tilde{t}_1}^2 + s_{2\theta_t}^2 m_{\tilde{t}_2}^2}{m_{\tilde{t}_1}^4} + \frac{s_{2\theta_t}^2}{m_{\tilde{t}_1}^4 m_{\tilde{t}_2}^2} \left( m_{\tilde{t}_1}^4 \ln \frac{m_{\tilde{t}_1}^2}{Q^2} - m_{\tilde{t}_2}^4 \ln \frac{m_{\tilde{t}_2}^2}{Q^2} \right) \right], \quad (28)$$

$$\frac{\partial Z^{4\tilde{t}}}{\partial m_{\tilde{t}_2}^2} = -\frac{C_F}{24} \left[ \frac{c_{2\theta_t}^2 m_{\tilde{t}_2}^2 + s_{2\theta_t}^2 m_{\tilde{t}_1}^2}{m_{\tilde{t}_2}^4} + \frac{s_{2\theta_t}^2}{m_{\tilde{t}_2}^4 m_{\tilde{t}_1}^2} \left( m_{\tilde{t}_2}^4 \ln \frac{m_{\tilde{t}_2}^2}{Q^2} - m_{\tilde{t}_1}^4 \ln \frac{m_{\tilde{t}_1}^2}{Q^2} \right) \right], \quad (29)$$

$$\frac{\partial Z^{4\tilde{t}}}{\partial c_{2\theta_t}^2} = -\frac{C_F}{24} \left[ \frac{(m_{\tilde{t}_1}^2 - m_{\tilde{t}_2}^2)^2}{m_{\tilde{t}_1}^2 m_{\tilde{t}_2}^2} - \frac{m_{\tilde{t}_1}^2 - m_{\tilde{t}_2}^2}{m_{\tilde{t}_2}^2} \ln \frac{m_{\tilde{t}_1}^2}{Q^2} - \frac{m_{\tilde{t}_2}^2 - m_{\tilde{t}_1}^2}{m_{\tilde{t}_1}^2} \ln \frac{m_{\tilde{t}_2}^2}{Q^2} \right], \quad (30)$$

where  $Q$  is the renormalization scale at which the  $\overline{\text{DR}}$  parameters in the one-loop form factors are expressed. Finally, the contributions of the two-loop diagrams that involve gluinos are somewhat longer and we report them in the appendix.

---

<sup>2</sup>Conversely, ref. [16] shows that, if the Higgs-squark-squark coupling is expressed in terms of the  $\overline{\text{MS}}$  Yukawa coupling, an additional two-loop contribution must be introduced.



### 3.2 Input parameters and renormalization schemes

To account for the case in which the parameters are expressed in a renormalization scheme different from  $\overline{\text{DR}}$ , we just have to shift the parameters appearing in the one-loop part of the form factors, after taking the limit of zero Higgs mass in the one-loop functions  $\mathcal{G}_0^{1\ell}$  and  $\mathcal{G}_{1/2}^{1\ell}$ . Since we are focusing on the two-loop QCD corrections we need to provide a renormalization prescription only for the top and stop masses, for the stop mixing angle, and for the soft SUSY-breaking trilinear coupling  $A_t$ . Indicating, generically, a quantity in the  $\overline{\text{DR}}$  scheme as  $x^{\overline{\text{DR}}}$ , and the same quantity in a generic scheme  $R$  as  $x^R$ , we can write the one-loop relation as  $x^{\overline{\text{DR}}} = x^R + \delta x$ . Then, if the one-loop form factors are evaluated in terms of  $R$  quantities, the two-loop functions in eqs. (21)–(24) must be replaced by

$$F_t^{2\ell} \longrightarrow F_t^{2\ell} + \frac{\pi}{6\alpha_s} \left[ \frac{\delta m_{\tilde{t}_1}^2}{m_{\tilde{t}_1}^4} - \frac{\delta m_{\tilde{t}_2}^2}{m_{\tilde{t}_2}^4} - \left( \frac{\delta m_t}{m_t} + \frac{\delta s_{2\theta_t}}{s_{2\theta_t}} \right) \left( \frac{1}{m_{\tilde{t}_1}^2} - \frac{1}{m_{\tilde{t}_2}^2} \right) \right], \quad (31)$$

$$G_t^{2\ell} \longrightarrow G_t^{2\ell} + \frac{\pi}{6\alpha_s} \left[ \frac{\delta m_{\tilde{t}_1}^2}{m_{\tilde{t}_1}^4} + \frac{\delta m_{\tilde{t}_2}^2}{m_{\tilde{t}_2}^4} - 2 \frac{\delta m_t}{m_t} \left( \frac{1}{m_{\tilde{t}_1}^2} + \frac{1}{m_{\tilde{t}_2}^2} \right) \right], \quad (32)$$

$$\tilde{F}_t^{2\ell} \longrightarrow \tilde{F}_t^{2\ell} + \frac{\pi}{6\alpha_s} \left[ \frac{\delta m_{\tilde{t}_1}^2}{m_{\tilde{t}_1}^4} - \frac{\delta m_{\tilde{t}_2}^2}{m_{\tilde{t}_2}^4} - \frac{\delta c_{2\theta_t}}{c_{2\theta_t}} \left( \frac{1}{m_{\tilde{t}_1}^2} - \frac{1}{m_{\tilde{t}_2}^2} \right) \right], \quad (33)$$

$$\tilde{G}_t^{2\ell} \longrightarrow \tilde{G}_t^{2\ell} + \frac{\pi}{6\alpha_s} \left[ \frac{\delta m_{\tilde{t}_1}^2}{m_{\tilde{t}_1}^4} + \frac{\delta m_{\tilde{t}_2}^2}{m_{\tilde{t}_2}^4} \right]. \quad (34)$$

In addition, the two-loop form factor  $\mathcal{H}_2^{2\ell}$  gets a contribution originating from the shift in  $A_t$ :

$$\mathcal{H}_2^{2\ell} \longrightarrow \mathcal{H}_2^{2\ell} - \frac{m_t s_{2\theta_t}}{s_\beta} \frac{\pi}{6\alpha_s} \left( \frac{1}{m_{\tilde{t}_1}^2} - \frac{1}{m_{\tilde{t}_2}^2} \right) \delta A_t. \quad (35)$$

A commonly adopted renormalization scheme for the input parameters is the so-called on-shell (OS) scheme, in which the top and stop parameters are related to physical quantities. In the OS scheme the top and stop masses are defined as the poles of the corresponding propagators, and the shifts w.r.t. the  $\overline{\text{DR}}$  scheme are

$$\delta m_t = \text{Re } \hat{\Sigma}_t(m_t), \quad \delta m_{\tilde{t}_1}^2 = \text{Re } \hat{\Pi}_{11}(m_{\tilde{t}_1}^2), \quad \delta m_{\tilde{t}_2}^2 = \text{Re } \hat{\Pi}_{22}(m_{\tilde{t}_2}^2), \quad (36)$$

where  $\hat{\Sigma}_t(m_t)$  and  $\hat{\Pi}_{ii}(m_{\tilde{t}_i}^2)$  denote the finite parts of the self-energies of top and stops, respectively, each computed at an external momentum equal to the corresponding particle's mass. Explicit formulae for the various shifts in eq. (36) can be found, e.g., in eqs. (B.2)–(B.4) of ref. [24]. For the shift in the stop mixing angle several OS definitions are possible. We choose  $\delta\theta_t$  in such a way that it cancels the anti-hermitian part of the stop wave-function renormalization (w.f.r.) matrix, leading to [29]

$$\delta\theta_t = \frac{1}{2} \frac{\hat{\Pi}_{12}(m_{\tilde{t}_1}^2) + \hat{\Pi}_{12}(m_{\tilde{t}_2}^2)}{m_{\tilde{t}_1}^2 - m_{\tilde{t}_2}^2}, \quad (37)$$

where  $\widehat{\Pi}_{12}(q^2)$  denotes the finite part of the off-diagonal self-energy of the stops, and is given in eq. (B.7) of ref. [24]. Finally, the trilinear coupling  $A_t$  is related to the other parameters in the top/stop sector by

$$s_{2\theta_t} = \frac{2m_t(A_t + \mu \cot \beta)}{m_{\tilde{t}_1}^2 - m_{\tilde{t}_2}^2}, \quad (38)$$

therefore, since  $\mu$  and  $\tan \beta$  do not get any  $\mathcal{O}(\alpha_s)$  correction, the shift for  $A_t$  is not an independent quantity and it can be expressed in terms of the other shifts:

$$\delta A_t = \left( \frac{\delta m_{\tilde{t}_1}^2 - \delta m_{\tilde{t}_2}^2}{m_{\tilde{t}_1}^2 - m_{\tilde{t}_2}^2} + \frac{\delta s_{2\theta_t}}{s_{2\theta_t}} - \frac{\delta m_t}{m_t} \right) (A_t + \mu \cot \beta). \quad (39)$$

We have verified that, in the OS scheme, the shifts in eqs. (31)–(35) cancel the explicit dependence of  $\mathcal{H}_1^{2\ell}$  and  $\mathcal{H}_2^{2\ell}$  on the renormalization scale  $Q$ .

We compared our results with those of the public computer code `evalcsusy.f`, which is based on the results of ref. [15]. The code provides the one- and two-loop parts of the Wilson coefficient for the Higgs-gluon-gluon operator in the effective Lagrangian, see eq. (2.1) and (2.5) of ref. [15], using an OS renormalization scheme for the parameters in the top/stop sector. After taking into account the different renormalization prescription for the stop mixing angle, the different convention for the sign of  $\mu$  in eq. (38), and an overall multiplicative factor in the normalization of the coefficients, we find *perfect* numerical agreement between our results and those of ref. [15]. However, we would like to comment on the renormalization prescription for the stop mixing angle adopted in ref. [15] (see also ref. [30]). Their counterterm is given by

$$\delta\theta_t = \frac{\Pi_{12}(q_0^2)}{m_{\tilde{t}_1}^2 - m_{\tilde{t}_2}^2}, \quad (40)$$

where  $q_0$  is an arbitrary external momentum (a free input parameter of `evalcsusy.f`) chosen to be of the order of the stop masses. The divergent part of the counterterm for  $\theta_t$  is indeed compelled to have the form of eq. (37) – with the finite part of the self-energy replaced by the divergent part – by the requirement that it cancel the poles of the anti-hermitian part of the stop w.f.r. matrix. The renormalization prescription given in eq. (40) fulfills this requirement in the case of the QCD corrections, because the divergent part of the  $\mathcal{O}(\alpha_s)$  contribution to  $\Pi_{12}(q^2)$  does not depend on  $q^2$ . In general, however, this is not the case, unless  $q_0^2 = (m_{\tilde{t}_1}^2 + m_{\tilde{t}_2}^2)/2$ . Therefore, we find it preferable to stick to the “symmetrical” prescription for  $\delta\theta_t$ , eq. (37), which can be more naturally applied to other loop corrections.

### 3.3 Contributions from squarks of other flavors

The results presented in the previous subsections are valid in the limit in which the Higgs boson mass is negligible with respect to the masses of the particles circulating in the loops. Therefore, care must be taken in extending the results derived for the top/stop contributions to the contributions of quarks

and squarks of other flavors. In the case of the bottom/sbottom contributions the general formulae of section 2 hold. However, the VHML can be strictly applied only to the two-loop contributions arising from diagrams with sbottoms and gluons, and to those arising from diagrams with quartic sbottom couplings. Results valid in the  $\overline{\text{DR}}$  scheme can be obtained for the former from eq. (27) and for the latter from eqs. (28)–(30), with the trivial substitution  $\tilde{t} \rightarrow \tilde{b}$  in the squark masses and mixing angle. Obviously, the VHML cannot be applied to the contributions arising from two-loop diagrams with bottom quarks and gluons, but the exact results for those contributions are available in the literature [4, 11, 12]. For what concerns the contributions of two-loop diagrams with bottom, sbottom and gluino, the VHML can only be applied under the further approximation that the bottom mass and the left-right mixing in the sbottom sector are set to zero (i.e.  $m_b = \theta_b = 0$ ), effectively killing the Yukawa-induced interactions between Higgs bosons and bottom (s)quarks. Since the left-right sbottom mixing contains a term proportional to  $m_b \tan \beta$ , this is not a good approximation when  $\tan \beta$  is large enough to offset the smallness of  $m_b$ .

When the bottom Yukawa coupling is neglected, the only diagrams that give a contribution to the form factors for the Higgs-gluon-gluon interaction are those in which the Higgs boson couples to the sbottoms through the electroweak, D-term-induced interaction. These diagrams contribute to the function  $D_b$  that appears in eqs. (11, 12) and is further decomposed into two functions  $\tilde{F}_b$  and  $\tilde{G}_b$  in eq. (13). The expressions in eqs. (23) and (24) for the two-loop part of the functions simplify to:

$$\tilde{F}_b^{2\ell} = \frac{\partial Z}{\partial m_{b_L}^2} - \frac{\partial Z}{\partial m_{b_R}^2}, \quad \tilde{G}_b^{2\ell} = \frac{\partial Z}{\partial m_{b_L}^2} + \frac{\partial Z}{\partial m_{b_R}^2}, \quad (41)$$

where, in the absence of left-right mixing, the sbottom mass eigenstates  $\tilde{b}_1$  and  $\tilde{b}_2$  are identified with  $\tilde{b}_L$  and  $\tilde{b}_R$ , respectively. The  $\overline{\text{DR}}$  contributions from the two-loop diagrams with gluons and with quartic sbottom coupling can again be read off eqs. (27)–(29) after replacing  $\tilde{t} \rightarrow \tilde{b}$  and setting  $\theta_b = 0$ . The contribution of the two-loop diagram with gluino, sbottom and (massless) bottom reads

$$\begin{aligned} \frac{\partial Z^{\tilde{g}}}{\partial m_{b_i}^2} &= -\frac{2 m_{\tilde{g}}^2}{3 m_{b_i}^4} C_F \left[ 1 - \log \frac{m_{\tilde{g}}^2}{Q^2} + \frac{m_{b_i}^4}{(m_{\tilde{g}}^2 - m_{b_i}^2)^2} \left( 2 + \frac{m_{\tilde{g}}^2 + m_{b_i}^2}{m_{\tilde{g}}^2 - m_{b_i}^2} \log \frac{m_{b_i}^2}{m_{\tilde{g}}^2} \right) \right] \\ &+ \frac{C_A}{3 (m_{\tilde{g}}^2 - m_{b_i}^2)} \left( 1 + \frac{m_{\tilde{g}}^2}{m_{\tilde{g}}^2 - m_{b_i}^2} \log \frac{m_{b_i}^2}{m_{\tilde{g}}^2} \right), \end{aligned} \quad (42)$$

where  $i = L, R$ . If the sbottom masses appearing in the one-loop part of the form factor are taken as the physical ones, the functions  $\tilde{F}_b^{2\ell}$  and  $\tilde{G}_b^{2\ell}$  must be shifted as in eqs. (33) and (34), neglecting the term proportional to  $\delta_{C_2\theta_b}$ . It is useful to remark that, as is clear from eq. (13), there is a partial cancellation between the sbottom contributions in  $D_b$  and the corresponding stop contributions in  $D_t$ . Therefore, the sbottom contributions controlled by the electroweak gauge couplings must be taken into account even when  $\tan \beta$  is small and the bottom Yukawa coupling can be neglected.

Finally, for the squarks of the first two generations the approximation of neglecting the Yukawa couplings is always satisfactory. The remaining D-term-induced contributions to the form factors can be obtained by trivially adapting the results in eqs. (27)–(29) and (42).

## 4 On the validity of the vanishing Higgs-mass limit

In the previous section we presented analytic results for the two-loop form factors  $\mathcal{H}_i^{2\ell}$  valid in the VHML. As already mentioned, we can expect this approximation to be quite good for the lightest CP-even Higgs boson  $h$ , while for the heaviest Higgs boson  $H$  it is probably less accurate. To put this expectation on a more solid ground we computed directly the two-loop top/stop contribution to the Higgs-gluon-gluon amplitude via a Taylor expansion in the external Higgs momentum up to terms of  $\mathcal{O}(m_\phi^2/M^2)$  – where  $\phi = h, H$ , and  $M$  denotes generically the masses of the heavy particles in the loop (i.e. top, stops and gluino). The validity of the Taylor expansion is restricted to Higgs masses below the first threshold that is encountered in the diagrams. This is always the case for  $h$ , while for  $H$  this situation is realized only in specific regions of the parameter space.

We computed the Higgs-gluon-gluon amplitude following the same strategy employed for the calculation of the gluon self-energy, see section 3.1. The zeroth-order term in the Taylor expansion reproduces the result that we obtained via the LET, while the  $\mathcal{O}(m_\phi^2/M^2)$  term in the expansion gives the first correction to the VHML. For simplicity we neglected all the (small) D-term-induced electroweak contributions. We expressed our results in the OS renormalization scheme outlined in section 3.2. We remark that, when converting to the OS scheme the results obtained originally in the  $\overline{\text{MS}}$  scheme, we must introduce additional two-loop contributions of  $\mathcal{O}(m_\phi^2/M^2)$ , originating from the shifts in the parameters that appear in the  $\mathcal{O}(m_\phi^2/M^2)$  parts of the one-loop form factors – see eq. (19). We checked that the additional contributions cancel the explicit renormalization-scale dependence of the  $\mathcal{O}(m_\phi^2/M^2)$  part of the two-loop form factors. The analytic expressions for the  $\mathcal{O}(m_\phi^2/M^2)$  corrections are very long and we do not report them.

Similarly to ref. [15], we present our results in two representative MSSM scenarios. The first scenario is the so-called SPS1a' slope [31], in which the soft SUSY-breaking parameters at the GUT scale are related as

$$m_0 = 0.28 m_{1/2}, \quad A_0 = -1.2 m_{1/2}, \quad (43)$$

where  $m_0$  and  $m_{1/2}$  are universal SUSY-breaking masses for scalars and gauginos, respectively,  $A_0$  is a universal Higgs-sfermion-sfermion interaction term, and the other relevant parameters are  $\tan\beta = 10$  and  $\mu < 0$  (with our sign convention). We vary the GUT-scale gaugino mass  $m_{1/2}$  between 100 GeV and 400 GeV, and the other SUSY-breaking parameters as in eq. (43) above. To compute the superparticle masses, we evolve the soft SUSY-breaking parameters down to the weak scale using the public computer code `SoftSusy` [32]. In the second scenario the light Higgs boson is “gluophobic”, i.e. the top quark contribution to the Higgs-gluon coupling is largely canceled by the contribution of a light stop. The scenario is defined directly in terms of weak-scale parameters, which we choose as

$$\tan\beta = 10, \quad \theta_t = \frac{\pi}{4}, \quad m_A = 300 \text{ GeV}, \quad \mu = -500 \text{ GeV}, \quad m_{\tilde{g}} = 500 \text{ GeV}, \quad m_{\tilde{t}_1} = 200 \text{ GeV}, \quad (44)$$

while  $m_{\tilde{t}_2}$  is varied between 250 GeV and 750 GeV. In the first scenario the CP-even Higgs masses and mixing angle are computed directly by `SoftSusy`, while in the second scenario we compute them using the two-loop  $\mathcal{O}(\alpha_t\alpha_s)$  results of ref. [24]. In both scenarios we take  $m_t = 172.6$  GeV [33].

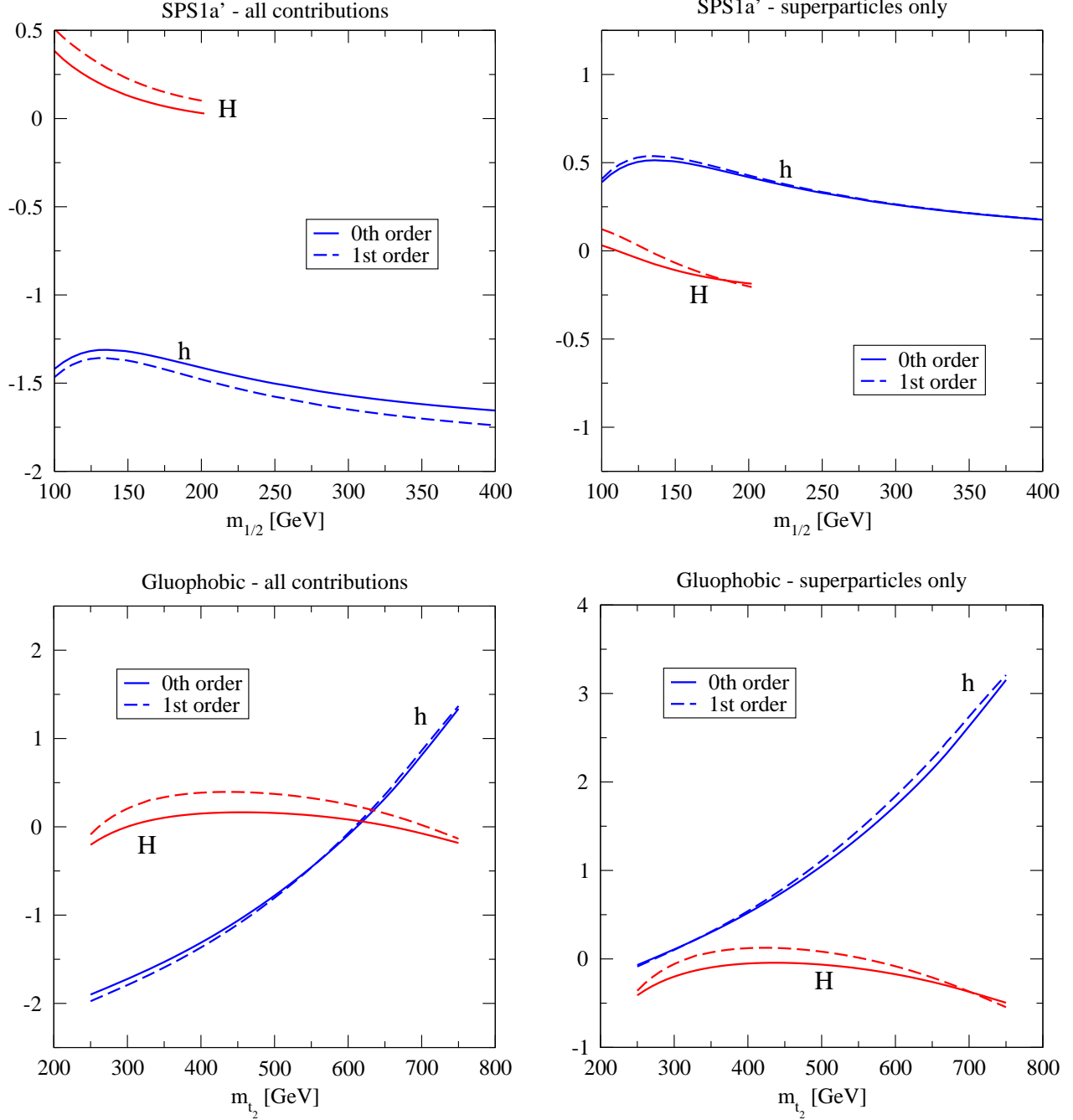


Figure 1: Two-loop form factors  $\mathcal{H}_h^{2\ell}$  and  $\mathcal{H}_H^{2\ell}$  in the SPS1a' scenario (upper plots) and in the gluophobic scenario (lower plots). The plots on the right include only the superparticle contributions. In each plot, the solid lines refer to the result obtained in the limit of vanishing Higgs mass, while the dashed lines include also terms of  $\mathcal{O}(m_\phi^2/M^2)$ . The lines for  $\mathcal{H}_H^{2\ell}$  in the SPS1a' scenario are truncated where  $m_H \approx 2m_t$ .

The four plots in figure 1 show our results for the two-loop form factors  $\mathcal{H}_h^{2\ell}$  and  $\mathcal{H}_H^{2\ell}$ , which we define as

$$\mathcal{H}_h^{2\ell} = T_F \left( -\sin \alpha \mathcal{H}_1^{2\ell} + \cos \alpha \mathcal{H}_2^{2\ell} \right), \quad \mathcal{H}_H^{2\ell} = T_F \left( \cos \alpha \mathcal{H}_1^{2\ell} + \sin \alpha \mathcal{H}_2^{2\ell} \right). \quad (45)$$

The two upper plots refer to the SPS1a' scenario, while the two lower plots refer to the gluophobic scenario. For each scenario, the plot on the left shows the complete two-loop top/stop contributions to the form factors, while the plot on the right shows only the contributions of the diagrams that include superparticles. Finally, for each Higgs boson  $\phi = h, H$ , the solid line corresponds to the result obtained for  $\mathcal{H}_\phi^{2\ell}$  in the VHML, while the dashed line includes also the contribution of the first-order term in the expansion in powers of  $m_\phi^2/M^2$ .

It can be seen from figure 1 that, for the lightest Higgs boson  $h$ , the corrections of  $\mathcal{O}(m_h^2/M^2)$  to the results obtained for  $\mathcal{H}_h^{2\ell}$  in the VHML are quite small, which should not come as a surprise since  $m_h$  is always considerably smaller than  $m_t$ . In the SPS1a' scenario, which as  $m_{1/2}$  increases is characterized by relatively heavy superparticles, the comparison between the plots on the left and right sides shows that the bulk of the corrections is contained in the diagrams with top quarks and gluons, for which a complete analytic result (i.e., valid for any value of the top and Higgs masses) is available [4, 11, 12]. In the gluophobic scenario there is still a small Higgs-mass dependence in the superparticle contribution, due to the presence of a relatively light stop. In summary, it appears to be quite safe to approximate the two-loop top and stop contributions to  $\mathcal{H}_h^{2\ell}$  with the results obtained via the LET in section 3. In case a more refined approximation is required, one can implement the complete result for the top/gluon contribution by replacing

$$\frac{\partial Z^g}{\partial m_t^2} \longrightarrow \frac{1}{2m_t^2} \left[ C_F \mathcal{G}_{1/2}^{(2\ell, C_R)} + C_A \mathcal{G}_{1/2}^{(2\ell, C_A)} \right], \quad (46)$$

in the gluonic part of the function  $G_t^{2\ell}$  defined in eq. (22). The functions  $\mathcal{G}_{1/2}^{(2\ell, C_R)}$  and  $\mathcal{G}_{1/2}^{(2\ell, C_A)}$  in the OS renormalization scheme are defined in eqs. (2.15) and (3.8) of ref. [12], respectively.

The situation is quite different for the heaviest Higgs boson  $H$ . As we mentioned before, the limit of vanishing  $m_H$  can only be considered if  $m_H$  is smaller than the lowest threshold appearing in the loops. Indeed, the curves for  $\mathcal{H}_H^{2\ell}$  in the SPS1a' scenario are truncated around  $m_{1/2} = 200$  GeV, where  $m_H$  approaches  $2m_t$ . On the other hand, it can be seen from figure 1 that, in the regions of the parameter space where the limit of vanishing  $m_H$  can be applied at all, the resulting approximation is not exceedingly bad even for  $m_H$  as large as 300 GeV. It should however be kept in mind that, in the case of large  $\tan \beta$ , the VHML approximation cannot be applied even if  $m_H$  is relatively small, because the  $H$  boson has enhanced couplings to the bottom (s)quarks (see the discussion in section 3.3). In that case a full computation is unavoidable [16].

## 5 Gluonic and photonic Higgs decays

The results of the previous sections can be directly applied to the NLO computation of the gluonic decay widths of the CP-even Higgs bosons in the MSSM. We specialize to the decay width of the  $h$  boson, but the formulae presented below can be applied also the decay of  $H$  using the replacements indicated at the end of section 2 (with the same restrictions outlined there and at the end of the previous section).

At NLO in QCD the decay width of the lightest Higgs boson in two gluons reads

$$\Gamma(h \rightarrow gg) = \frac{G_\mu \alpha_s (\mu_R)^2 m_h^3}{16 \sqrt{2} \pi^3} \left| T_F \left( -\sin \alpha \mathcal{H}_1^{1\ell} + \cos \alpha \mathcal{H}_2^{1\ell} \right) \right|^2 \left( 1 + \frac{\alpha_s}{\pi} \mathcal{C} \right), \quad (47)$$

where  $\mathcal{C} = \mathcal{C}_{virt} + \mathcal{C}_{ggg} + \mathcal{C}_{gq\bar{q}}$  includes contributions from the two-loop virtual corrections and from the one-loop real radiation processes  $h \rightarrow ggg$ ,  $h \rightarrow gq\bar{q}$ . The contribution of the two-loop virtual corrections is straightforwardly obtained from the results of the previous sections:

$$\mathcal{C}_{virt} = C_A \frac{\pi^2}{3} + \beta_0 \ln \left( \frac{\mu_R^2}{m_h^2} \right) + \left( \frac{-\sin \alpha \mathcal{H}_1^{2\ell} + \cos \alpha \mathcal{H}_2^{2\ell}}{-\sin \alpha \mathcal{H}_1^{1\ell} + \cos \alpha \mathcal{H}_2^{1\ell}} + \text{h.c.} \right), \quad (48)$$

while the contributions of the real radiation processes are, in the VHML,

$$C_{ggg} = -C_A \left( \frac{\pi^2}{3} + \frac{73}{12} \right), \quad C_{gq\bar{q}} = -\frac{7}{6} N_f, \quad (49)$$

where  $N_f$  is the number of light quark species, with the quarks treated as massless particles.

Considering for illustration the two scenarios described in section 4, we found that the numerical value of the last term (within parentheses) in the r.h.s. of eq. (48) is approximately  $-2.6 C_F + 2.5 C_A$  in the SPS1a' scenario with  $m_{1/2} = 200$  GeV, and  $-4.5 C_F + 2.8 C_A$  in the gluophobic scenario with  $m_{\tilde{t}_2} = 500$  GeV. For the heaviest Higgs boson the corresponding values are  $-2.9 C_F + 1.4 C_A$  (SPS1a') and  $-1.1 C_F + 0.9 C_A$  (gluophobic). In both scenarios the superparticle contribution to the coefficient of  $C_F$  is comparable to the corresponding SM contribution, while the superparticle contribution to the coefficient of  $C_A$  is much smaller than its SM counterpart.

As a byproduct of our calculation, we can also provide the explicit results for the two-loop QCD corrections to the quark/squark contributions to the photonic Higgs decay. The partial width for the decay of the lightest CP-even Higgs boson  $h$  in two photons can be written as

$$\Gamma(h \rightarrow \gamma\gamma) = \frac{G_\mu \alpha_{em}^2 m_h^3}{128 \sqrt{2} \pi^3} \left| -\sin \alpha \mathcal{P}_1 + \cos \alpha \mathcal{P}_2 \right|^2, \quad (50)$$

where  $\alpha_{em}$  is the electromagnetic coupling and  $\mathcal{P}_i$  ( $i = 1, 2$ ) are defined, in analogy to the  $\mathcal{H}_i$  in eq. (3), as the form factors for the coupling of the neutral, CP-even component of the Higgs doublet  $H_i$  with two photons. At one loop, the form factors  $\mathcal{P}_1$  and  $\mathcal{P}_2$  receive contributions from all the electrically charged states of the MSSM (see, e.g., the first paper in ref. [4] for the explicit results) and they are in general dominated by the contribution of the diagram involving the  $W$  boson. However, only the

contributions involving quarks and squarks receive QCD corrections at two loops. We separate the one-loop part of the form factors and the two-loop QCD corrections as

$$\mathcal{P}_i = \mathcal{P}_i^{1\ell} + \frac{\alpha_s}{\pi} \mathcal{P}_i^{2\ell} + \dots, \quad (51)$$

where the ellipses stand for three-loop terms of  $\mathcal{O}(\alpha_s^2)$  and for two-loop terms controlled by other coupling constants.

Focusing on the contributions of the third-generation quarks and squarks,  $\mathcal{P}_1$  and  $\mathcal{P}_2$  can be decomposed exactly as in eqs. (11) and (12), with the following substitutions in the r.h.s. of eqs. (11) and (12)

$$F_q \rightarrow \widehat{F}_q, \quad G_q \rightarrow \widehat{G}_q, \quad D_q \rightarrow \widehat{D}_q, \quad \lambda_t \rightarrow \frac{Q_t^2 N_c}{\sin \beta}, \quad \lambda_b \rightarrow \frac{Q_b^2 N_c}{\cos \beta} \quad (52)$$

where  $Q_q$  is the electric charge of the quark. With our overall normalization we have for the functions entering the one-loop parts of the form factors,  $\mathcal{P}_i^{1\ell}$ ,

$$\widehat{F}_q^{1\ell} = F_q^{1\ell}, \quad \widehat{G}_q^{1\ell} = G_q^{1\ell}, \quad \widehat{D}_q^{1\ell} = D_q^{1\ell}, \quad (53)$$

while for the ones entering  $\mathcal{P}_i^{2\ell}$

$$\widehat{F}_q^{2\ell} = F_q^{2\ell} \Big|_{C_A=0}, \quad \widehat{G}_q^{2\ell} = G_q^{2\ell} \Big|_{C_A=0}, \quad \widehat{D}_q^{2\ell} = D_q^{2\ell} \Big|_{C_A=0}, \quad (54)$$

i.e. the functions entering the two-loop parts of the form factors can be obtained by setting  $C_A = 0$  in the results presented in section 3 and in the appendix.

## 6 Discussion

The LET allowed us to derive explicit and compact analytical formulae, for the top/stop contributions to the form factors for the interaction of a CP-even Higgs boson with two gluons, valid in the limit in which the mass of the Higgs boson is neglected w.r.t. the masses of the particles running in the loops. By direct inspection of the first correction to the results obtained in the VHML, we have argued that, for the lightest MSSM Higgs boson, the VHML results provide a quite good approximation to the full result, whereas for the heaviest Higgs boson the approximation is less good, and can be applied only in specific regions of the parameter space. For what concerns the sbottom contributions to the form factors, the validity of our results is limited to the case of small or moderate  $\tan \beta$ .

As mentioned in section 3.1, the form factor for the interaction of a CP-odd Higgs boson  $A$  with two gluons receives an additional contribution from the axial-current anomaly and cannot be computed in the same way as the form factors for the CP-even bosons (indeed, the first derivatives of the gluon self-energy w.r.t. the CP-odd parts of the Higgs fields vanish at the minimum of the Higgs potential). In the VHML the  $A$ -gluon-gluon form factor does not receive any contribution beyond one loop from diagrams involving gluons [34], as a consequence of the Adler-Bardeen theorem [35]. However, there is



a non-vanishing two-loop contribution from the diagrams involving gluinos which requires an explicit diagrammatic calculation [36].

Finally, the LET can also be applied to multiple Higgs boson production [22]. By taking multiple derivatives of the gluon self-energy w.r.t. the CP-even or CP-odd Higgs fields, it is indeed possible to compute the SUSY-QCD corrections to the production of any number of CP-even Higgs bosons and of any even number of CP-odd Higgs bosons in the VHML. The simplest case would be the calculation of the SUSY-QCD corrections to the pair production of both CP-even and CP-odd Higgs bosons. An analysis of these processes, restricted to the top-quark contributions, has been presented in ref. [37].

## Acknowledgments

We thank C. Anastasiou and G. Ridolfi for useful discussions. This work was supported in part by an EU Marie-Curie Research Training Network under contract MRTN-CT-2006-035505 and by ANR under contract BLAN07-2\_194882.

## Appendix

We provide in this appendix the explicit expressions for the contributions of the two-loop diagrams with top, stop and gluino to the derivatives of  $Z$ . For every derivative we separate the coefficients of the color factors  $C_F$  and  $C_A$  as

$$\frac{\partial Z^{\tilde{g}}}{\partial x_i} = C_F \frac{\partial Z_{C_F}^{\tilde{g}}}{\partial x_i} + C_A \frac{\partial Z_{C_A}^{\tilde{g}}}{\partial x_i}, \quad (\text{A1})$$

for  $x_i = (m_t^2, m_{\tilde{t}_1}^2, m_{\tilde{t}_2}^2, c_{2\theta_t}^2)$ . In terms of the two-loop function  $\Phi(x, y, z)$  defined, e.g., in the appendix A of ref. [27], and using the shortcut  $\Delta \equiv m_{\tilde{g}}^4 + m_{\tilde{t}_1}^4 + m_t^4 - 2(m_{\tilde{g}}^2 m_{\tilde{t}_1}^2 + m_{\tilde{g}}^2 m_t^2 + m_{\tilde{t}_1}^2 m_t^2)$ , the contributions to the various derivatives<sup>3</sup> read

$$\begin{aligned} \frac{\partial Z_{C_F}^{\tilde{g}}}{\partial m_{\tilde{t}_1}^2} &= \frac{1}{6 m_{\tilde{t}_1}^4 \Delta^2} \left[ (m_{\tilde{g}}^2 + m_t^2) \Delta^2 + 2 m_{\tilde{g}}^2 m_{\tilde{t}_1}^4 (\Delta + 10 m_{\tilde{g}}^2 m_t^2) \right] \\ &- \frac{m_{\tilde{g}} s_{2\theta_t}}{6 m_t m_{\tilde{t}_1}^4 \Delta^2} \left[ m_t^2 \Delta^2 + 2 m_{\tilde{t}_1}^4 (\Delta + 5 m_{\tilde{g}}^2 m_t^2) (m_{\tilde{g}}^2 + m_t^2 - m_{\tilde{t}_1}^2) \right] \\ &- \frac{m_{\tilde{g}}^4}{6 m_{\tilde{t}_1}^4 \Delta^3} \log \frac{m_{\tilde{g}}^2}{m_t^2} \left\{ (m_{\tilde{g}}^2 - m_t^2 - 4 m_{\tilde{t}_1}^2) \Delta^2 \right. \\ &\quad \left. + 2 m_{\tilde{t}_1}^2 \left( -18 m_t^2 m_{\tilde{t}_1}^2 \Delta + ((3 m_t^2 - m_{\tilde{g}}^2) \Delta - 30 m_{\tilde{g}}^2 m_t^2 m_{\tilde{t}_1}^2) (m_t^2 - m_{\tilde{g}}^2 + m_{\tilde{t}_1}^2) \right) \right. \\ &\quad \left. - \frac{s_{2\theta_t}}{m_{\tilde{g}} m_t} \left[ 2 m_{\tilde{t}_1}^2 (m_{\tilde{t}_1}^2 + m_t^2) + m_t^2 (m_{\tilde{g}}^2 - m_t^2) \right] \Delta^2 \right. \\ &\quad \left. - 2 m_t^2 m_{\tilde{t}_1}^2 \left( -9 m_{\tilde{g}}^2 m_{\tilde{t}_1}^2 \Delta + ((2 m_{\tilde{g}}^2 - 9 m_{\tilde{t}_1}^2) \Delta - 30 m_{\tilde{g}}^2 m_t^2 m_{\tilde{t}_1}^2) (m_{\tilde{g}}^2 - m_t^2 + m_{\tilde{t}_1}^2) \right) \right] \left. \right\} \\ &+ \frac{m_{\tilde{g}}^2}{6 \Delta^3} \log \frac{m_{\tilde{t}_1}^2}{m_t^2} \left\{ \Delta^2 + 12 m_{\tilde{g}}^2 m_t^2 \Delta + (2 m_{\tilde{t}_1}^2 \Delta + 60 m_{\tilde{g}}^2 m_t^2 m_{\tilde{t}_1}^2) (m_t^2 + m_{\tilde{g}}^2 - m_{\tilde{t}_1}^2) \right. \\ &\quad \left. - \frac{2 s_{2\theta_t}}{m_{\tilde{g}} m_t} \left[ (m_{\tilde{g}}^2 + m_t^2) \Delta^2 + m_{\tilde{g}}^2 m_t^2 (3 m_{\tilde{g}}^2 + 3 m_t^2 + 20 m_{\tilde{t}_1}^2) \Delta + 60 m_{\tilde{g}}^4 m_t^4 m_{\tilde{t}_1}^2 \right] \right\} \\ &- \frac{1}{6 m_{\tilde{t}_1}^4} \left( m_{\tilde{g}}^2 + m_t^2 - s_{2\theta_t} m_{\tilde{g}} m_t \right) \log \frac{m_t^2}{Q^2} \\ &+ \frac{m_{\tilde{g}}^4 m_t^2}{m_{\tilde{t}_1}^2 \Delta^3} \Phi(m_{\tilde{g}}^2, m_t^2, m_{\tilde{t}_1}^2) \left\{ (m_{\tilde{g}}^2 + m_t^2 + 3 m_{\tilde{t}_1}^2) \Delta + 20 m_{\tilde{g}}^2 m_t^2 m_{\tilde{t}_1}^2 \right. \\ &\quad \left. - \frac{s_{2\theta_t}}{m_{\tilde{g}} m_t} \left[ \Delta^2 + 2 m_{\tilde{g}}^2 m_t^2 \Delta + (3 m_{\tilde{t}_1}^2 \Delta + 10 m_{\tilde{g}}^2 m_t^2 m_{\tilde{t}_1}^2) (m_{\tilde{g}}^2 + m_t^2 - m_{\tilde{t}_1}^2) \right] \right\}, \quad (\text{A2}) \end{aligned}$$

---

<sup>3</sup>  $\partial Z^{\tilde{g}}/\partial m_{\tilde{t}_2}^2$  can be obtained from  $\partial Z^{\tilde{g}}/\partial m_{\tilde{t}_1}^2$  through the replacements  $\tilde{t}_1 \rightarrow \tilde{t}_2$  and  $s_{2\theta_t} \rightarrow -s_{2\theta_t}$ .

$$\begin{aligned}
\frac{\partial Z_{CA}^{\tilde{g}}}{\partial m_{\tilde{t}_1}^2} &= \frac{1}{12 \Delta^2} \left[ 2 m_t^2 \Delta - (\Delta + 20 m_{\tilde{g}}^2 m_t^2) (m_{\tilde{g}}^2 - m_t^2 - m_{\tilde{t}_1}^2) \right] \\
&+ \frac{m_t s_{2\theta_t}}{3 m_{\tilde{g}} \Delta^2} \left[ 2 m_{\tilde{g}}^2 \Delta - (\Delta + 5 m_{\tilde{g}}^2 m_t^2) (m_t^2 - m_{\tilde{g}}^2 - m_{\tilde{t}_1}^2) \right] \\
&+ \frac{m_{\tilde{g}}^2}{12 \Delta^3} \log \frac{m_{\tilde{g}}^2}{m_{\tilde{t}_1}^2} \left\{ \Delta^2 + 2 m_t^2 \left( (13 m_{\tilde{g}}^2 + 9 m_t^2 + 15 m_{\tilde{t}_1}^2) \Delta + 120 m_{\tilde{g}}^2 m_t^2 m_{\tilde{t}_1}^2 \right) \right. \\
&\quad \left. - \frac{2 s_{2\theta_t} m_t}{m_{\tilde{g}}} \left[ 18 m_t^2 (m_t^2 - m_{\tilde{t}_1}^2) \Delta \right. \right. \\
&\quad \quad \left. \left. + \left( (11 m_{\tilde{g}}^2 - 9 m_t^2 + 9 m_{\tilde{t}_1}^2) \Delta + 60 m_{\tilde{g}}^2 m_t^2 m_{\tilde{t}_1}^2 \right) (m_{\tilde{g}}^2 + m_t^2 - m_{\tilde{t}_1}^2) \right] \right\} \\
&- \frac{m_t^2}{12 \Delta^3} \log \frac{m_t^2}{m_{\tilde{t}_1}^2} \left\{ 12 m_t^2 (m_{\tilde{t}_1}^2 - m_t^2) \Delta \right. \\
&\quad \left. + \left( (15 m_{\tilde{g}}^2 + 13 m_t^2 + 3 m_{\tilde{t}_1}^2) \Delta + 120 m_{\tilde{g}}^2 m_t^2 m_{\tilde{t}_1}^2 \right) (m_{\tilde{g}}^2 + m_t^2 - m_{\tilde{t}_1}^2) \right. \\
&\quad \left. - \frac{4 s_{2\theta_t}}{m_{\tilde{g}} m_t} \left[ (3 m_{\tilde{g}}^2 + m_t^2) \Delta^2 + m_{\tilde{g}}^2 m_t^2 \left( (9 m_{\tilde{g}}^2 + 2 m_t^2 + 21 m_{\tilde{t}_1}^2) \Delta + 60 m_{\tilde{g}}^2 m_t^2 m_{\tilde{t}_1}^2 \right) \right] \right\} \\
&+ \frac{m_{\tilde{g}}^2 m_t^2}{2 m_{\tilde{t}_1}^2 \Delta^3} \Phi(m_{\tilde{g}}^2, m_t^2, m_{\tilde{t}_1}^2) \left\{ 2 m_t^2 m_{\tilde{t}_1}^2 \Delta \right. \\
&\quad \left. + \left( (m_{\tilde{g}}^2 + m_t^2 + 2 m_{\tilde{t}_1}^2) \Delta + 20 m_{\tilde{g}}^2 m_t^2 m_{\tilde{t}_1}^2 \right) (m_t^2 - m_{\tilde{g}}^2 + m_{\tilde{t}_1}^2) \right. \\
&\quad \left. + \frac{s_{2\theta_t}}{m_{\tilde{g}} m_t} \left[ (m_{\tilde{g}}^2 - m_t^2 + m_{\tilde{t}_1}^2) \Delta^2 + 2 m_t^2 \left( 2 m_{\tilde{t}_1}^2 (m_t^2 - m_{\tilde{t}_1}^2) \Delta \right. \right. \right. \\
&\quad \quad \left. \left. + \left( (m_{\tilde{g}}^2 + 5 m_{\tilde{t}_1}^2) \Delta + 10 m_{\tilde{g}}^2 m_t^2 m_{\tilde{t}_1}^2 \right) (m_{\tilde{g}}^2 - m_t^2 + m_{\tilde{t}_1}^2) \right] \right\}, \quad (A3)
\end{aligned}$$

$$\begin{aligned}
\frac{\partial Z_{CF}^{\tilde{g}}}{\partial m_t^2} &= -\frac{m_{\tilde{g}}^2}{6 m_{\tilde{t}_1}^2 \Delta^2} \left[ 4 m_{\tilde{t}_1}^2 \Delta + (\Delta - 10 m_{\tilde{g}}^2 m_{\tilde{t}_1}^2) (m_{\tilde{g}}^2 - m_t^2 - m_{\tilde{t}_1}^2) \right] \\
&- \frac{m_{\tilde{g}} s_{2\theta_t}}{12 m_t m_{\tilde{t}_1}^2 \Delta^2} \left[ \Delta^2 + 2 \left( 5 m_{\tilde{g}}^2 m_{\tilde{t}_1}^2 \Delta + \left( (2 m_{\tilde{t}_1}^2 - m_{\tilde{g}}^2) \Delta + 10 m_{\tilde{g}}^2 m_t^2 m_{\tilde{t}_1}^2 \right) (m_{\tilde{g}}^2 - m_t^2 + m_{\tilde{t}_1}^2) \right) \right] \\
&+ \frac{m_{\tilde{g}}^4}{6 m_{\tilde{t}_1}^2 \Delta^3} \log \frac{m_{\tilde{g}}^2}{m_t^2} \left\{ \Delta^2 - 2 m_{\tilde{t}_1}^2 \left( (2 m_{\tilde{g}}^2 + 3 m_t^2 + 9 m_{\tilde{t}_1}^2) \Delta + 60 m_{\tilde{g}}^2 m_t^2 m_{\tilde{t}_1}^2 \right) \right. \\
&\quad \left. - \frac{s_{2\theta_t}}{2 m_{\tilde{g}} m_{\tilde{t}_1}^3} \left[ (m_t^4 - 2 m_{\tilde{t}_1}^4 + m_{\tilde{g}}^2 (m_t^2 + 2 m_{\tilde{t}_1}^2)) \Delta^2 + m_{\tilde{t}_1}^2 m_{\tilde{t}_1}^2 \left( 20 m_{\tilde{g}}^2 m_t^2 \Delta \right. \right. \right.
\end{aligned}$$

$$\begin{aligned}
& -((25 m_{\tilde{t}_1}^2 + 9 m_{\tilde{g}}^2 + 11 m_t^2) \Delta + 120 m_{\tilde{g}}^2 m_t^2 m_{\tilde{t}_1}^2)(m_{\tilde{g}}^2 + m_t^2 - m_{\tilde{t}_1}^2) \Big] \Big\} \\
& + \frac{m_{\tilde{g}}^2 m_{\tilde{t}_1}^2}{3 \Delta^3} \log \frac{m_{\tilde{t}_1}^2}{m_t^2} \left\{ 9 m_{\tilde{g}}^2 \Delta + (\Delta + 30 m_{\tilde{g}}^2 m_t^2) (m_{\tilde{g}}^2 - m_t^2 + m_{\tilde{t}_1}^2) \right. \\
& \quad + \frac{s_{2\theta_t}}{2 m_{\tilde{g}} m_t^3} \left[ (m_{\tilde{g}}^2 + 3 m_t^2 - m_{\tilde{t}_1}^2) \Delta^2 \right. \\
& \quad \quad \left. \left. + m_{\tilde{g}}^2 m_t^2 (12 m_t^2 \Delta + (17 \Delta + 60 m_{\tilde{g}}^2 m_t^2) (m_t^2 - m_{\tilde{g}}^2 + m_{\tilde{t}_1}^2)) \right] \right\} \\
& + \frac{1}{6 m_{\tilde{t}_1}^2} \left( 1 - \frac{s_{2\theta_t} m_{\tilde{g}}}{2 m_t} \right) \log \frac{m_t^2}{Q^2} \\
& - \frac{m_{\tilde{g}}^4}{\Delta^3} \Phi(m_{\tilde{g}}^2, m_t^2, m_{\tilde{t}_1}^2) \left\{ 2 m_t^2 \Delta + (\Delta + 10 m_{\tilde{g}}^2 m_t^2) (m_t^2 - m_{\tilde{g}}^2 + m_{\tilde{t}_1}^2) \right. \\
& \quad \left. + \frac{s_{2\theta_t}}{2 m_{\tilde{g}} m_t} \left[ \Delta^2 + 2 m_t^2 (3 m_{\tilde{g}}^2 \Delta + (3 \Delta + 10 m_{\tilde{g}}^2 m_t^2) (m_{\tilde{g}}^2 - m_t^2 + m_{\tilde{t}_1}^2)) \right] \right\} \\
& + (\tilde{t}_1 \rightarrow \tilde{t}_2, \quad s_{2\theta_t} \rightarrow -s_{2\theta_t}), \tag{A4}
\end{aligned}$$

$$\begin{aligned}
\frac{\partial Z_{CA}^{\tilde{g}}}{\partial m_t^2} & = -\frac{1}{12 \Delta^2} \left[ (5 m_{\tilde{g}}^2 + 5 m_{\tilde{t}_1}^2 - m_t^2) \Delta + 40 m_{\tilde{g}}^2 m_t^2 m_{\tilde{t}_1}^2 \right] \\
& - \frac{s_{2\theta_t}}{12 m_{\tilde{g}} m_t \Delta^2} \left[ 10 m_t^2 (m_{\tilde{t}_1}^2 - m_t^2) \Delta \right. \\
& \quad \left. + \left( (8 m_t^2 - 5 m_{\tilde{g}}^2 - 2 m_{\tilde{t}_1}^2) \Delta - 20 m_{\tilde{g}}^2 m_t^2 m_{\tilde{t}_1}^2 \right) (m_t^2 + m_{\tilde{g}}^2 - m_{\tilde{t}_1}^2) \right] \\
& - \frac{m_{\tilde{g}}^2}{12 \Delta^3} \log \frac{m_{\tilde{g}}^2}{m_t^2} \left\{ \Delta^2 + 12 m_t^2 m_{\tilde{t}_1}^2 \Delta \right. \\
& \quad \left. + \left( (4 m_{\tilde{g}}^2 + 18 m_{\tilde{t}_1}^2) \Delta + 120 m_{\tilde{g}}^2 m_t^2 m_{\tilde{t}_1}^2 \right) (m_t^2 - m_{\tilde{g}}^2 + m_{\tilde{t}_1}^2) \right\} \\
& \quad + \frac{s_{2\theta_t}}{m_{\tilde{g}} m_t} \left[ (m_{\tilde{g}}^2 + 4 m_t^2 + 12 m_{\tilde{t}_1}^2) \Delta^2 + 4 m_t^2 \left( 16 m_{\tilde{t}_1}^2 (m_t^2 - m_{\tilde{t}_1}^2) \Delta \right. \right. \\
& \quad \left. \left. + (m_t^2 + 24 m_{\tilde{t}_1}^2) \Delta + 30 m_{\tilde{g}}^2 m_t^2 m_{\tilde{t}_1}^2 \right) (m_{\tilde{g}}^2 - m_t^2 + m_{\tilde{t}_1}^2) \right] \Big\} \\
& - \frac{m_{\tilde{t}_1}^2}{12 \Delta^3} \log \frac{m_{\tilde{t}_1}^2}{m_t^2} \left\{ 8 m_t^2 (m_{\tilde{t}_1}^2 - m_t^2) \Delta \right. \\
& \quad \left. + \left( (19 m_{\tilde{g}}^2 + 9 m_t^2 + 3 m_{\tilde{t}_1}^2) \Delta + 120 m_{\tilde{g}}^2 m_t^2 m_{\tilde{t}_1}^2 \right) (m_{\tilde{g}}^2 + m_t^2 - m_{\tilde{t}_1}^2) \right\} \\
& \quad - \frac{s_{2\theta_t}}{m_{\tilde{g}} m_t} \left[ (11 m_{\tilde{g}}^2 + 2 m_t^2 + 2 m_{\tilde{t}_1}^2) \Delta^2 \right]
\end{aligned}$$

$$\begin{aligned}
& + 2 m_{\tilde{g}}^2 m_t^2 \left( (21 m_{\tilde{g}}^2 + 3 m_t^2 + 43 m_{\tilde{t}_1}^2) \Delta + 120 m_{\tilde{g}}^2 m_t^2 m_{\tilde{t}_1}^2 \right) \Big\} \\
- & \frac{m_{\tilde{g}}^2}{2 \Delta^3} \Phi(m_{\tilde{g}}^2, m_t^2, m_{\tilde{t}_1}^2) \left\{ \Delta^2 + m_t^2 \left( (7 m_{\tilde{g}}^2 + 7 m_{\tilde{t}_1}^2 + m_t^2) \Delta + 40 m_{\tilde{g}}^2 m_t^2 m_{\tilde{t}_1}^2 \right) \right. \\
& - \frac{s_{2\theta_t}}{2 m_{\tilde{g}} m_t} \left[ (m_{\tilde{g}}^2 + 3 m_t^2 - m_{\tilde{t}_1}^2) \Delta^2 + 2 m_t^2 \left( 2 m_{\tilde{t}_1}^2 (m_{\tilde{t}_1}^2 - m_t^2) \Delta \right. \right. \\
& \left. \left. + ((3 m_{\tilde{g}}^2 + 2 m_t^2 + 6 m_{\tilde{t}_1}^2) \Delta + 20 m_{\tilde{g}}^2 m_t^2 m_{\tilde{t}_1}^2) (m_{\tilde{g}}^2 + m_t^2 - m_{\tilde{t}_1}^2) \right) \right] \Big\} \\
+ & (\tilde{t}_1 \rightarrow \tilde{t}_2, \quad s_{2\theta_t} \rightarrow -s_{2\theta_t}), \tag{A5}
\end{aligned}$$

$$\begin{aligned}
\frac{\partial Z_{CF}^{\tilde{g}}}{\partial c_{2\theta_t}^2} &= \frac{m_t m_{\tilde{g}}}{12 s_{2\theta_t} m_{\tilde{t}_1}^2 \Delta} \left( 2 m_{\tilde{g}}^2 m_{\tilde{t}_1}^2 - \Delta \right) \\
& + \frac{m_{\tilde{g}}^3}{12 s_{2\theta_t} m_t m_{\tilde{t}_1}^2 \Delta^2} \left[ 4 m_t^2 m_{\tilde{t}_1}^2 \Delta \right. \\
& \left. + \left( (2 m_{\tilde{t}_1}^2 - m_t^2) \Delta + 6 m_{\tilde{g}}^2 m_t^2 m_{\tilde{t}_1}^2 \right) (m_t^2 - m_{\tilde{g}}^2 + m_{\tilde{t}_1}^2) \right] \log \frac{m_{\tilde{g}}^2}{m_t^2} \\
& + \frac{m_{\tilde{g}} m_{\tilde{t}_1}^2}{6 s_{2\theta_t} m_t \Delta^2} (\Delta + 3 m_{\tilde{g}}^2 m_t^2) (m_{\tilde{g}}^2 + m_t^2 - m_{\tilde{t}_1}^2) \log \frac{m_{\tilde{t}_1}^2}{m_t^2} + \frac{m_{\tilde{g}} m_t}{12 s_{2\theta_t} m_{\tilde{t}_1}^2} \log \frac{m_t^2}{Q^2} \\
& + \frac{m_{\tilde{g}}^3 m_t}{2 s_{2\theta_t} \Delta^2} (\Delta + 2 m_{\tilde{g}}^2 m_t^2) \Phi(m_{\tilde{g}}^2, m_t^2, m_{\tilde{t}_1}^2) \\
& + (\tilde{t}_1 \rightarrow \tilde{t}_2, \quad s_{2\theta_t} \rightarrow -s_{2\theta_t}),
\end{aligned}$$

$$\begin{aligned}
\frac{\partial Z_{CA}^{\tilde{g}}}{\partial c_{2\theta_t}^2} &= \frac{m_t m_{\tilde{g}}}{12 s_{2\theta_t} \Delta} (m_t^2 + m_{\tilde{t}_1}^2 - m_{\tilde{g}}^2) \\
& + \frac{m_{\tilde{g}} m_t}{12 s_{2\theta_t} \Delta^2} \left( (m_{\tilde{g}}^2 + 6 m_{\tilde{t}_1}^2) \Delta + 12 m_{\tilde{g}}^2 m_t^2 m_{\tilde{t}_1}^2 \right) \log \frac{m_{\tilde{g}}^2}{m_t^2} \\
& - \frac{m_t m_{\tilde{t}_1}^2}{12 s_{2\theta_t} m_{\tilde{g}} \Delta^2} \left[ 3 m_{\tilde{g}}^2 \Delta + \left( 2 \Delta + 6 m_{\tilde{g}}^2 m_t^2 \right) (m_{\tilde{g}}^2 - m_t^2 + m_{\tilde{t}_1}^2) \right] \log \frac{m_{\tilde{t}_1}^2}{m_t^2} \\
& - \frac{m_{\tilde{g}} m_t}{4 s_{2\theta_t} \Delta^2} \left[ (\Delta + 2 m_{\tilde{g}}^2 m_t^2) (m_{\tilde{g}}^2 - m_t^2 - m_{\tilde{t}_1}^2) \right] \Phi(m_{\tilde{g}}^2, m_t^2, m_{\tilde{t}_1}^2) \\
& + (\tilde{t}_1 \rightarrow \tilde{t}_2, \quad s_{2\theta_t} \rightarrow -s_{2\theta_t}). \tag{A6}
\end{aligned}$$

## References

- [1] A. Djouadi, Phys. Rept. **457** (2008) 1 [arXiv:hep-ph/0503172], Phys. Rept. **459** (2008) 1 [arXiv:hep-ph/0503173].
- [2] H. M. Georgi, S. L. Glashow, M. E. Machacek and D. V. Nanopoulos, Phys. Rev. Lett. **40** (1978) 692.
- [3] S. Dawson, Nucl. Phys. B **359** (1991) 283; A. Djouadi, M. Spira and P. M. Zerwas, Phys. Lett. B **264** (1991) 440.
- [4] M. Spira, A. Djouadi, D. Graudenz and P. M. Zerwas, Nucl. Phys. B **453** (1995) 17 [arXiv:hep-ph/9504378]; R. Harlander and P. Kant, JHEP **0512** (2005) 015 [arXiv:hep-ph/0509189].
- [5] R. V. Harlander, Phys. Lett. B **492** (2000) 74. [arXiv:hep-ph/0007289]; S. Catani, D. de Florian and M. Grazzini, JHEP **0105** (2001) 025 [arXiv:hep-ph/0102227]; R. V. Harlander and W. B. Kilgore, Phys. Rev. D **64** (2001) 013015 [arXiv:hep-ph/0102241], Phys. Rev. Lett. **88** (2002) 201801 [arXiv:hep-ph/0201206]; C. Anastasiou and K. Melnikov, Nucl. Phys. B **646** (2002) 220 [arXiv:hep-ph/0207004]; V. Ravindran, J. Smith and W. L. van Neerven, Nucl. Phys. B **665** (2003) 325 [arXiv:hep-ph/0302135].
- [6] S. Catani, D. de Florian, M. Grazzini and P. Nason, JHEP **0307** (2003) 028 [arXiv:hep-ph/0306211].
- [7] S. Moch and A. Vogt, Phys. Lett. B **631** (2005) 48 [arXiv:hep-ph/0508265].
- [8] A. Djouadi and P. Gambino, Phys. Rev. Lett. **73** (1994) 2528 [arXiv:hep-ph/9406432]; A. Djouadi, P. Gambino and B. A. Kniehl, Nucl. Phys. B **523** (1998) 17 [arXiv:hep-ph/9712330].
- [9] U. Aglietti, R. Bonciani, G. Degrossi and A. Vicini, Phys. Lett. B **595** (2004) 432 [arXiv:hep-ph/0404071], Phys. Lett. B **600** (2004) 57 [arXiv:hep-ph/0407162]; G. Degrossi and F. Maltoni, Phys. Lett. B **600** (2004) 255 [arXiv:hep-ph/0407249].
- [10] S. Dawson, A. Djouadi and M. Spira, Phys. Rev. Lett. **77** (1996) 16 [arXiv:hep-ph/9603423].
- [11] C. Anastasiou, S. Beerli, S. Bucherer, A. Daleo and Z. Kunszt, JHEP **0701** (2007) 082 [arXiv:hep-ph/0611236].
- [12] U. Aglietti, R. Bonciani, G. Degrossi and A. Vicini, JHEP **0701** (2007) 021 [arXiv:hep-ph/0611266].
- [13] M. Muhlleitner and M. Spira, Nucl. Phys. B **790** (2008) 1 [arXiv:hep-ph/0612254].
- [14] R. V. Harlander and M. Steinhauser, Phys. Lett. B **574** (2003) 258 [arXiv:hep-ph/0307346].

- [15] R. V. Harlander and M. Steinhauser, *JHEP* **0409** (2004) 066 [arXiv:hep-ph/0409010].
- [16] C. Anastasiou, S. Beerli and A. Daleo, arXiv:0803.3065 [hep-ph].
- [17] M. A. Shifman, A. I. Vainshtein, M. B. Voloshin and V. I. Zakharov, *Sov. J. Nucl. Phys.* **30** (1979) 711 [*Yad. Fiz.* **30** (1979) 1368];
- [18] R. Bonciani, G. Degrossi and A. Vicini, *JHEP* **0711** (2007) 095 [arXiv:0709.4227 [hep-ph]].
- [19] R. K. Ellis, I. Hinchliffe, M. Soldate and J. J. van der Bij, *Nucl. Phys. B* **297** (1988) 221.
- [20] U. Baur and E. W. N. Glover, *Nucl. Phys. B* **339** (1990) 38.
- [21] G. Degrossi, S. Heinemeyer, W. Hollik, P. Slavich and G. Weiglein, *Eur. Phys. J. C* **28** (2003) 133 [arXiv:hep-ph/0212020]; B. C. Allanach, A. Djouadi, J. L. Kneur, W. Porod and P. Slavich, *JHEP* **0409** (2004) 044 [arXiv:hep-ph/0406166].
- [22] B. A. Kniehl and M. Spira, *Z. Phys. C* **69** (1995) 77 [arXiv:hep-ph/9505225].
- [23] L. F. Abbott, *Nucl. Phys. B* **185** (1981) 189; A. Denner, G. Weiglein and S. Dittmaier, *Nucl. Phys. B* **440** (1995) 95 [hep-ph/9410338].
- [24] G. Degrossi, P. Slavich and F. Zwirner, *Nucl. Phys. B* **611** (2001) 403 [arXiv:hep-ph/0105096].
- [25] T. Hahn, *Comput. Phys. Commun.* **140** (2001) 418 [arXiv:hep-ph/0012260]; T. Hahn and C. Schappacher, *Comput. Phys. Commun.* **143** (2002) 54 [arXiv:hep-ph/0105349].
- [26] A. I. Davydychev and J. B. Tausk, *Nucl. Phys. B* **397** (1993) 123.
- [27] A. Dedes and P. Slavich, *Nucl. Phys. B* **657** (2003) 333 [arXiv:hep-ph/0212132].
- [28] S. P. Martin and M. T. Vaughn, *Phys. Lett. B* **318** (1993) 331 [arXiv:hep-ph/9308222].
- [29] A. Pilaftsis, *Nucl. Phys. B* **504** (1997) 61 [arXiv:hep-ph/9702393]; J. Guasch, J. Sola and W. Hollik, *Phys. Lett. B* **437** (1998) 88 [arXiv:hep-ph/9802329]; H. Eberl, S. Kraml and W. Majerotto, *JHEP* **9905** (1999) 016 [arXiv:hep-ph/9903413]; Y. Yamada, *Phys. Rev. D* **64** (2001) 036008 [hep-ph/0103046].
- [30] A. Djouadi, P. Gambino, S. Heinemeyer, W. Hollik, C. Junger and G. Weiglein, *Phys. Rev. D* **57** (1998) 4179 [arXiv:hep-ph/9710438].
- [31] B. C. Allanach *et al.*, *Eur. Phys. J. C* **25** (2002) 113 [hep-ph/0202233]; J. A. Aguilar-Saavedra *et al.*, hep-ph/0511344.
- [32] B. C. Allanach, *Comput. Phys. Commun.* **143** (2002) 305 [arXiv:hep-ph/0104145].
- [33] CDF and D0 Collaborations, arXiv:0803.1683 [hep-ex].

- [34] R. P. Kauffman and W. Schaffer, Phys. Rev. D **49** (1994) 551 [arXiv:hep-ph/9305279]; A. Djouadi, M. Spira and P. M. Zerwas, Phys. Lett. B **311** (1993) 255 [arXiv:hep-ph/9305335]; M. Spira, A. Djouadi, D. Graudenz and P. M. Zerwas, Phys. Lett. B **318** (1993) 347.
- [35] S. L. Adler and W. A. Bardeen, Phys. Rev. **182** (1969) 1517.
- [36] R. V. Harlander and F. Hofmann, JHEP **0603** (2006) 050 [arXiv:hep-ph/0507041].
- [37] S. Dawson, S. Dittmaier and M. Spira, Phys. Rev. D **58** (1998) 115012 [arXiv:hep-ph/9805244].